Van Hove singularities and spectral smearing in high-temperature superconducting H_{3}S

Yundi Quan and Warren E. Pickett

Phys. Rev. B **93**, 104526 — Published 25 March 2016

DOI: 10.1103/PhysRevB.93.104526

van Hove singularities and spectral smearing in high temperature superconducting H_3S

Yundi Quan and Warren E. Pickett*
Department of Physics, University of California Davis, Davis, California 95616, USA
(Dated: January 20, 2016)

The superconducting phase of hydrogen sulfide at T_c=200 K observed by Drozdov and collaborators at pressures around 200 GPa is simple bcc $Im\bar{3}m$ H_3S, from a combination of theoretical and experimental confirmation. The various "extremes" that are involved – high pressure implying extreme reduction of volume, extremely high H phonon energy scale around 1400K, extremely high temperature for a superconductor – necessitates a close look at new issues raised by these characteristics in relation to high T_c itself. First principles methods are applied to analyze the H_3S electronic structure, beginning with the effect of sulfur and then focusing on the origin and implications of the two van Hove singularities (vHs) providing an impressive peak in the density of states near the Fermi energy. Implications arising from strong coupling Migdal-Eliashberg theory are studied. It becomes evident that electron spectral density smearing due to virtual phonon emission and absorption must be accounted for in a correct understanding of this unusual materials, and to obtain accurate theoretical predictions. Means for increasing T_c in H_3S-like materials are noted.

I. INTRODUCTION

The recent discovery of superconducting hydrogen sulfide under high pressure by Drozdov and collaborators[1–3], and remarkably predicted a year earlier by Duan *et al.*,[4] has reinvigorated the quest for room temperature superconductivity. The predicted structure has been confirmed by x-ray diffraction studies by Einaga *et al.*[5] that show that sulfur lies on a bcc sublattice; the protons cannot be seen in x-ray diffraction. The resistivity transitions were also confirmed by Einaga *et al.*. The experimental reports indicate critical temperatures up to T_c=203 K in the pressure range of 200 GPa, based on the resistivity transition, the effect of magnetic field on T_c, on a H isotope shift of the right sign and roughly the expected magnitude,[1] and the Meissner effect has been demonstrated.[2]

In a success of predictive theory in this area, the magnitude of T_c in the 200 GPa pressure range was obtained from first principles calculation *prior to experiment*[4] and confirmed by others,[6,7,10] so there can be little doubt that 200 K superconductivity has been achieved in the structurally simple compound H_3S, pictured in Fig. 1. The finding that H vibrations provide the mechanism seems to confirm the suggestion of Ashcroft that dense hydrogen should superconduct at high temperature,[11] however evidence is increasing that H-rich materials[12] are substantially different and more promising than pure hydrogen until TPa pressures can be reached. Early quantitative estimates[13] of T_c for metallic H were in the 250K range; more recent values[14] for pressures of several TPa lie in the 500-750K range. The phase diagram of this system is uncertain, however, due to the quantum nature of the proton.

Although comprehensive calculations based on density functional theory (DFT) linear response formalism and Eliashberg theory[15] have been reported and seem convincing, H_3S turns out to be more intricate than the initial reports suggest. Using their self-consistent harmonic approximation, Errea *et al.*[6] find substantial corrections due to anharmonicity: at 200 GPa, anharmonicity increases the characteristic frequency ω_{log} by 3%, the electron-phonon interaction (EPI) strength λ is decreased by 30% and the predicted value of T_c falls 22% from 250 K to 194 K. Potentially important for further understanding is their finding that anharmonicity shifts coupling strength to H-S bond stretch modes, from H-S bond bending (alternatively, H-H bond stretch) modes.

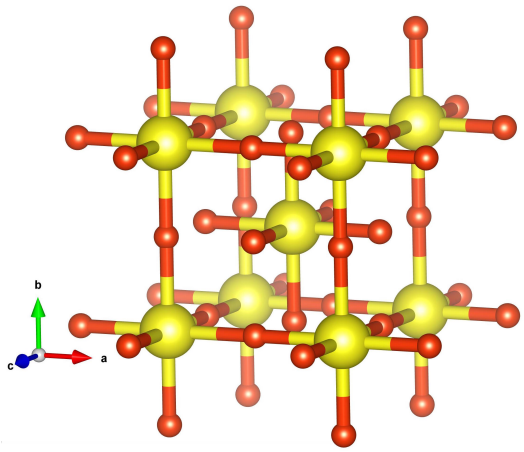

FIG. 1: Crystal structure of $Im\bar{3}m$ H_3S. Nearest neighbor S-H bonds are shown. At this nearest neighbor level, the structure consists of two interleaved ReO_3 sublattices, displaced relative to one another by the body-centering vector $(1,1,1)a/2$.

Other basic questions have yet to be addressed. First, why are the electron-phonon matrix elements as large as they are? While the main causative property behind the high T_c is the (understandably) high phonon frequencies that set the energy scale for T_c, substantial electron-ion matrix elements are also required. Second, Flores-Livas *et al.*[10] have investigated the energy dependence of the spectrum around the Fermi level, finding that it

influences the theoretical predictions, which are overly optimistic when energy dependence is neglected. Both Akashi *et al.*[16] and Flores-Livas *et al.* have solved the gap equations, providing theoretical predictions of the gap as well as T_c without using the Allen-Dynes equation. The questions posed by intricacies in the density of states (DOS) and the role of zero point vibrations has stimulated work by Bianconi and Jarlborg.[17]

More fundamentally there is the question "why H_3S? why sulfur?" Several H-rich materials have been studied at high pressure (see references in Refs. [4,6,7,10] and Bernstein *et al.*[8]), and although some are predicted to superconduct up to several tens of kelvins, H_3S is a singular standout. Li *et al.*,[18] for example, studied the H_2S stoichiometry for stable compounds up to similar high pressures, finding a maximum T_c of "only" 80 K. There is little understanding so far of the microscopic cause of very high T_c, beyond the obvious expectation of higher phonon frequencies at high pressure; the origin of the large matrix elements remain obscure. Papaconstantopoulos and collaborators[7] calculated the pressure dependence of matrix elements, finding increasing H scattering with increasing pressure. More basically one can ask, is there something special about sulfur, and the underlying electronic structure, that provides the platform for such high T_c?

It is the last of these questions we address initially in this paper. An obvious feature for study is the strikingly sharp peak in the density of states $N(E)$ due to two van Hove singularities (vHs) separated by 300 meV very near the Fermi level E_F. There is a large literature on the connection between peaks in $N(E)$ and high T_c in the A15 class of materials[19] and later in the high temperature superconducting cuprates,[20,21] but their importance for H_3S is unclear. van Hove singularities near the Fermi level can enhance $N(E_F)$ and thus the electron-phonon coupling strength λ due to increased number of available states to participate, but there are additional questions to address.

The paper is organized as follows. Methods are described in a brief Sec. II. In Sec. III the general electronic structure and the charge density near E_F are presented and discussed. The two van-Hove singularities are identified, quantified, and analyzed, and the relation between them is identified. In Section IV we address the peak in N(E) in the light of strong electron-phonon coupling (EPC), high frequencies, and thermal and EPC-induced smearing. Sec. V presents scenarios for further increase in coupling strength λ, and raising of T_c toward room temperature, in this and similar systems. A short Summary is provided in Sec. VI.

II. METHODS

Density functional calculations have been carried out using both the linearized augmented plane wave (LAPW) method based Wien2k code[22] and the linear combination of atomic orbitals based FPLO code.[23] The PBE implementation[24] of the generalized gradient approximation (GGA) is used as the exchange correlation functional. Except where noted, the results will be those from Wien2k. The crystal structure of H_3S is $Im\bar{3}m$ with a lattice constant of 5.6 a.u. corresponding[7] to a pressure of 210 GPa. All atoms lie at high symmetry sites.

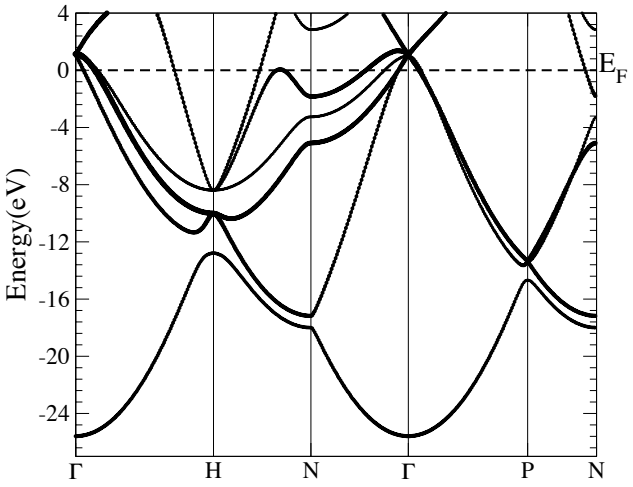

FIG. 2: (Color online) DFT band structure of H_3S at a=5.6 a.u., with the Fermi level set to zero. The darker bands in the -10 eV to +4 eV region have more H 1s character than the others. The position of the van Hove singularity discussed in the text is not visible along these symmetry lines.

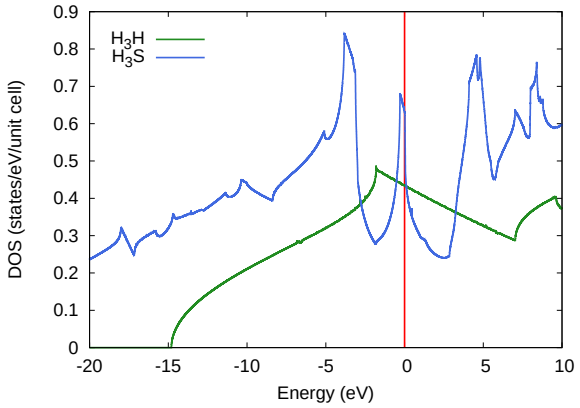

FIG. 3: Density of states of H_3S compared to that of H3H at the same volume, from Wien2k calculation. The bandwidth is extremely large due to the broadening caused by short interatomic distances. The peak in $N(E)$ arises from two van Hove singularities within 300 meV of each other and occurring in the region of the Fermi energy. $N(E_F)$=0.63 states/eV for H_3S. The impact of H bonding with the S 3p orbitals is evident.

To study the vHs points near the Fermi level, a very fine k-mesh containing 8094 in the irreducible Brillouin zone is used. Sphere radii R for H and S are 0.97 a_0 and 1.81 a_0 respectively, with basis set cutoff determined by $R_H K_{max} = 6$. The results we discuss are insensitive to these choices. The tight-binding parameters we present were obtained from projection to symmetry-adapted Wannier functions as implemented in FPLO.

III. ELECTRONIC STRUCTURE

The calculated lattice constant[7] at 210 GPa, a=5.6 a.u. corresponding to a volume 58% of the zero pressure volume in the same structure, is used in all calculations. The rather simple band structure of H_3S is shown in Fig. 2 and, up to some differences near the Fermi level, is consistent with previous work.[4,8,9] The very large occupied bandwidth of 26 eV reflects both the nearly free electron aspects of the the lower part of the valence bands, with this aspect being enhanced by the reduced volume that increases electron density and hopping amplitudes. Both effects increase the bandwidth: the reduced volume increases the density and hence elevates the Fermi energy, also the increased bandwidth reflects increased hopping amplitudes. Several bands cross the Fermi level, with varying velocities.

The DOS $N(E)$ on a broad scale is presented in Fig. 3. The occupied bandwidth is 26 eV. Over the lowest 20 eV of this range, the DOS has a remarkably free-electron-like $\sqrt{E}$ shape, without significant structure. Over the lower end of this region, the DOS is dominated by S 3s character, above which H 1s and S 3p character enter and mix. Then, at -4 eV and +5 eV two substantial and rather narrow peaks emerge, indicative of very strong hybridization, presumably being bonding and antibonding signatures. Double valleys lie at -2 eV and +2 eV, between which a very sharp peak, related to two van Hove singularities (vHs) 300 meV apart in energy, juts upward. The Fermi energy E_F (set to zero throughout) lies very near the upper vHs. The vHs are discussed further in Sec. III.D.

Papaconstantopoulos *et al.* provided[7] the orbital projected DOS for H_3S. The lower peak, at -4 eV, is very strongly S 3p in character, while the sharp peak at E_F is a strong mixture of S 3p with H 1s. The upper peak at +5 eV is a mixture of these two characters with states of more planewave-like character. We note that the shape of the DOS in Fig. 3 is significantly different than that of Duan *et al.*,[4] in spite of the similarity of the bands along symmetry directions.

We demonstrate in Sec. IV that for physical superconducting properties, thermal and, more importantly, dynamical broadening makes details of N(E) fine structure unimportant in some respects. This unimportance *does not however apply* for the underlying theory based on the static lattice, where it has serious consequences as discussed in Sec. V. Briefly, the issue is that so much in conventional EPC theory is formulated and evaluated in terms of the specific value of $N(E_F)$ assuming N(E) is slowly varying, which is not the case in H_3S.

A. Importance of Sulfur

As one clear means to assess the effect of H-S orbital mixing, Fig. 3 displays $N(E)$ also for a hypothetical material, H_3H, in which the S atom is replaced by H in the same structure. The spectrum is very different in a wide range around the Fermi level. Unusually, an almost perfectly linear region of $N(E)$ extends between two vHs 9 eV apart, on opposite sides and far from the Fermi level. The point however is that the strong structure in H_3S in the -4 eV to +5 eV region is missing in H_3H. The hypothetical nature of H_3H, which is in fact a simple cubic lattice of hydrogen, is corroborated by our calculation of the phonon spectrum, which results in many imaginary frequencies signaling dynamic instability.

Returning to the H_3S DOS, such strong structure in N(E) reflects strong mixing between orbitals lying in this energy range, which are the H 1s and S 3p valence orbitals. The orbital projected DOS (PDOS) presented by Papaconstantopoulos *et al.*[7] shows that S 3s participation is becoming small around E_F. Their PDOS helps to understand the strong DOS structure. The peak at -4 eV is largely S 3p character with some H 1s contribution. The peak at +5 eV has, surprisingly, a large contribution from Bloch orbitals with d symmetry around the S site, with some participation of all of the orbitals besides S s. The peak at E_F – the important one bounded by two closely spaced vHs – is a strong mixture of H 1s with S 3p, whose corresponding tight binding hopping parameters will have a correspondingly large hopping amplitude.

We also compare in Fig. 4 N(E) for H_3X, X=P and Cl, to that of H_3S, aligned at the H_3S band filling. Despite some variation in the on-site 3p energy and electronegativity, N(E) is quite similar among the three. The peak in N(E) at E_F is narrower for both P and Cl, i.e. the vHs are closer together. The strength of the peak at E_F appears to decrease somewhat from P→Cl. The distinction of S is that it places the band filling at the peak in N(E).

To quantify H-S hybridization relative to that of H-H, symmetry projected Wannier functions (WFs) were calculated using the FPLO code, projecting on S 3s and 3p, and H 1s atomic orbitals, for a total of seven WFs per primitive cell. The WF basis provides a tight binding representation of the DFT bands over a 30+ eV region, although requiring hopping parameters out to several neighbors. We denote the sulfur states by S and P and the H orbital by s in the subscripts of the hopping integrals. The WFs are pictured in Fig. 5, with both S 3p and H 1s WFs showing anisotropy and extension, reflecting the strong H-S mixing.

The on-site energies and largest Slater-Koster parameters are listed in Table I. Relative to E_F=0, the on-

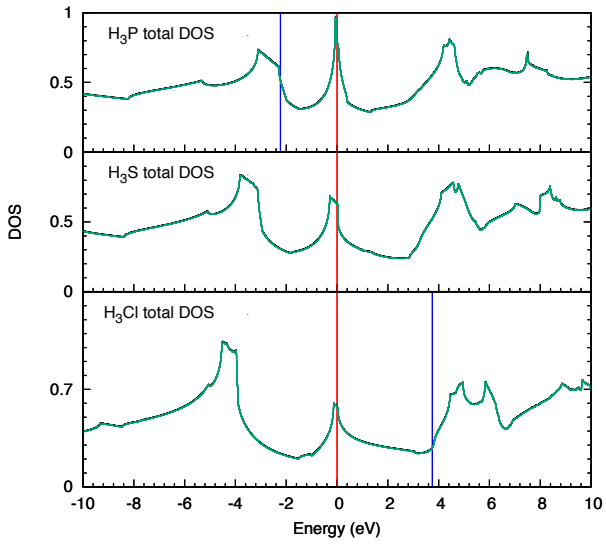

FIG. 4: Density of states (per eV-f.u.) of the sequence H_3X, X=P, S, Cl, aligned at the band filling of H_3S. The Fermi levels of H_3P and H_3Cl (using the H_3S structure, hence hypothetical) are shown by the vertical lines at appropriate band fillings. The similarity is striking; a rigid band (or virtual crystal) picture of alloys near H_3S holds qualitatively.

TABLE I: Selected tight-binding hopping amplitudes (in eV) from the transformation to Wannier functions.The subscripts indicate the index of the neighbor: 1≡1st neighbor, 2≡2nd neighbor, etc. For H there are two 4th neighbors one lattice constant apart: one through the S atom, denoted "4," one through another H atom, denoted "4′." $(\widetilde{PP})_1$ indicates $\frac{1}{4}(PP\sigma)_1 + \frac{3}{4}(PP\pi)_1$, which only occurs in this combination.

ϵ_S	-7.98	$(sP\sigma)_1$	-5.42
ϵ_s	-5.46	$(PP\sigma)_2$	-1.83
ϵ_P	-0.03	$(SP\sigma)_2$	1.29
$(sS\sigma)_1$	-4.37	$(SS\sigma)_2$	0.94
$(ss\sigma)_1$	-2.80	$(sP\sigma)_2$	-0.93
$(ss\sigma)_4$	-1.14	$(\widetilde{PP})_1$	0.60
$(ss\sigma)'_4$	0.55	$(SS\sigma)_1$	0.30

site energies (compared to those reported by Bernstein *et al.*[8], provided here in parentheses) are: ε_S =-8.0 (-8.6) eV; ε_s =-5.5 (-5.0) eV; ε_P = 0.03 (-1.3) eV. The procedures used by Bernstein *et al.* are not exactly the same as ours, with the difference indicating the level of confidence one should assign to these site energies considering the non-uniqueness of tight binding representations. It is eye-catching that our sulfur P on-site energy is indistinguishable from E_F.

The largest hopping parameters (Table I) are nearest neighbor (n.n.) $sP\sigma$ (-5.4 eV) and $sS\sigma$ (-4.4 eV), the former confirming that H-S n.n. hopping is dominant in creating the DOS structure. We have calculated the DOS for a single sublattice, which is ReO_3-structure H_3S, and it is nothing like the full DOS. The n.n. H-H hopping $ss\sigma$, at -2.8 eV, couples the sublattices strongly, and S-S second neighbor hoppings, one lattice constant apart, are 1.3-1.8 eV in magnitude. Interesting are the 4th neighbor H-H hoppings, between atoms one lattice constant apart. The hopping through the S atom $(ss\sigma)_4$ is -1.1 eV, while through an intervening H atom $(ss\sigma)'_4$ is half that size with opposite sign.

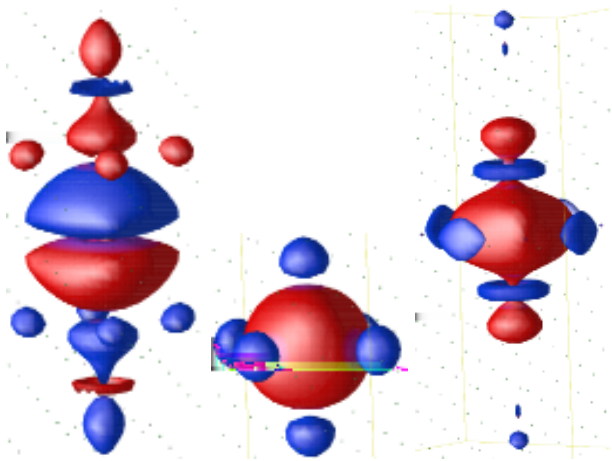

FIG. 5: Left: sulfur $3p_z$ Wannier function, showing strong mixing with H $1s$ contributions above and below. Center: sulfur $3s$ Wannier function, with minor hybridization to neighboring $1s$ orbitals. Right: hydrogen centered Wannier function, revealing strong hybridization of H $1s$ with S $3p\sigma$ above and below,, as well as mixing with neighboring H $1s$ orbitals along the other two axes.

As mentioned, the peak in N(E) reveals that the band filling in H_3S happens to be almost perfect for large response to perturbations, with E_F lying within the sharp peak. Retaining the same band filling suggests substituting Se or Te for S. Flores-Livas *et al.*[10] have done parallel calculations for H_3S and H_3Se. The H_3Se frequency ω_{log} is 10% *higher* but the calculated value of λ is lower by 40%, with the resulting T_c being lower by 27%. The changes of ω_{log} and λ indicate that the product $\eta = N(E_F) < I^2 >$ (not reported) is lower by 20% for the Se compound. Here $< I^2 >$ is the Fermi surface average of the square of the electron-H ion scattering matrix element. With H so dominant in the EPC and H modes separated from S (or Se) modes, electron-phonon coupling and superconductivity is dominated[7] by the H contribution

$$\lambda_H = \frac{N(E_F) < I_H^2 >}{M_H \omega_H^2}, \qquad (1)$$

where the matrix element refers to scattering from the displaced H potential and ω_H is a characteristic frequency from H modes.

The other isovalent "chalcogenide" is oxygen, which is quite different from S chemically with H. We have found that the DOS of H_3O in the H_3S structure differs substantially from that of H_3S. It may be relevant that H_2O does not metalize until *much higher* pressures than are being considered here. Heil and Boeri[9] have considered

bonding, EPC, and T_c where sulfur is alloyed with other group VI atoms. With alloying treated in the virtual crystal approximation (averaging pseudopotentials), they have suggested that a more electronegative ion will help. This leaves only oxygen in that column, and they calculated that a strong increase in matrix elements compensates a considerable decrease in $N(E_F)$, so that λ might increase somewhat. Ge *et al.* have also suggested partial replacement[25] of S, with P being the most encouraging, due to the increase in $N(E_F)$.

While S changes the electronic system very substantially from that of H_3H and its T_c is spectacular, it may not be so special. A variety of calculations have predicted (see Durajski *et al.*[27] for references) high values of T_c (in parentheses) for H-rich solids: $SiH_4(H_2)_2$ (107 K at 250 GPa), B_2H_6H (147 K at 360 GPa), Si_2H_6 (174 K at 275 GPa), CaH_6 (240 K at 150 GPa). Whether any general principles can be extracted from these results remains to be determined.

B. Charge density within 1eV of Fermi level

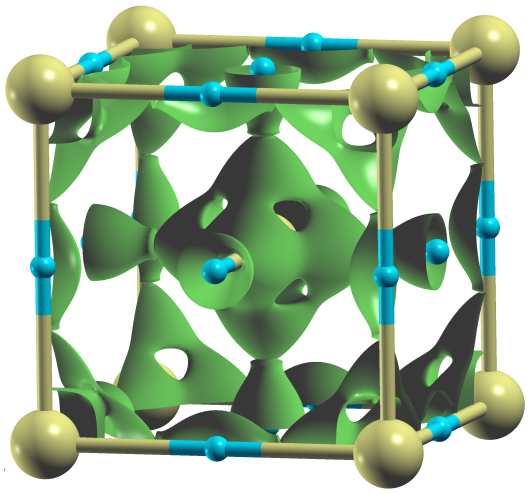

FIG. 6: Isosurface of the charge density obtained from states in the energy range $E_F \pm 1$ eV. Sulfur atoms (yellow spheres) lie at the corners and at the body center, H atom are denoted by small blue spheres.

The charge density from states within 1 eV of E_F is shown in Fig. 6; it is this density whose coupling to H vibrations gives strong coupling and the very high value of T_c. Results from smaller energy slices are no different, indicating that the states in this range have the same character. The density around S is strongly distorted from spherical symmetry, having substantial maxima in the direction of neighboring H atoms. The H density is strongly elongated toward the two neighboring S atoms. These shapes reflect strong covalent H $1s$ - S $3p_\sigma$ interaction discussed above. There remains a density minimum in the bond center rather than a bond charge maximum. This character is typical of strong directional bonding in metallic compounds.

C. van Hove singularities of H_3S

N(E) the energy range -1.0 eV to 0.2 eV was fit to the following piecewise expression[26] for 3D vHs near two singularities at energies $\epsilon_{lo} < \epsilon_{hi}$

$$N(E) = \begin{cases} a_1\sqrt{|b_1 - \epsilon|} + c_1\epsilon + d_1 & \epsilon < \epsilon_{lo} \\ a_2\epsilon + b_2 & \epsilon_{lo} < \epsilon < \epsilon_{hi} \\ a_3\sqrt{|\epsilon + b_3|} + c_3\epsilon + d_3 & \epsilon_{hi} < \epsilon \end{cases} \quad (2)$$

Energy isosurfaces at the two vHs energies are presented in Fig. 7. The vHs points lie at either end of a line where low velocity regions of two sheets of Fermi surface break apart at the zone boundary, and then "unzip" until they separate into disjoint sheets. The vHs (from the FPLO bands) at -0.43 eV occurs at $(-0.42, 0.21, 0)\pi/a$ and symmetric points. In the local principal axis coordinate system the effective masses are $-0.15m_e$, $1.36m_e$, $0.14m_e$, giving a thermal (or DOS) mass $m_{th} \equiv |m_1 m_2 m_3|^{1/3} = 0.31m_e$. The thermal mass is one measure of the strength of the vHs. For the one at -0.11 eV, the masses are $-0.83m_e$, $-0.16m_e$, $0.56m_e$, and m_{th}=$0.42m_e$. We return to the importance of vHs effective masses in Sec. V.

IV. IMPACT OF DYNAMICAL ELECTRON-PHONON INTERACTION

Thermal broadening as described by the Fermi-Dirac distribution function has well understood consequences, and is a factor in determining (in limiting) T_c, though it is usually not thermal broadening of the DOS, which is normally constant over an energy range of several $k_B T_c$. The purely thermal aspect is formalized in the gap to thermal broadening scale ratio $2\Delta/\pi k_B T_c \approx 1$, and is central to, but standard in, Eliashberg theory. Specifically, it is thermally excited electron and hole quasiparticles that overcome pairing and restores the normal state above T_c.

However, the sharp structure in N(E) on the scale of relevant phonon energies requires an extension of conventional implementations of Eliashberg theory.[15] Conventionally, a constant N(E) on the phonon energy scale is assumed, so all scattering processes can be considered as confined to the Fermi surface E=E_F. This issue was confronted long ago,[28,29] because of the sharp structure in N(E) in several of the then-high-T_c A15 structure compounds, viz. Nb_3Sn, V_3Si, Nb_3Ge, with $T_c \sim 20$ K, and has been followed up in related applications.[30,31]

In H_3S around 200 GPa, the representative frequency is $\Omega \sim 1300$ K $= 112$ meV. We have chosen this value based on the DFT-based calculations of (harmonic) ω_{log} frequencies ranging from 1125 K to 1450 K. [4,6,9,10,16,25],

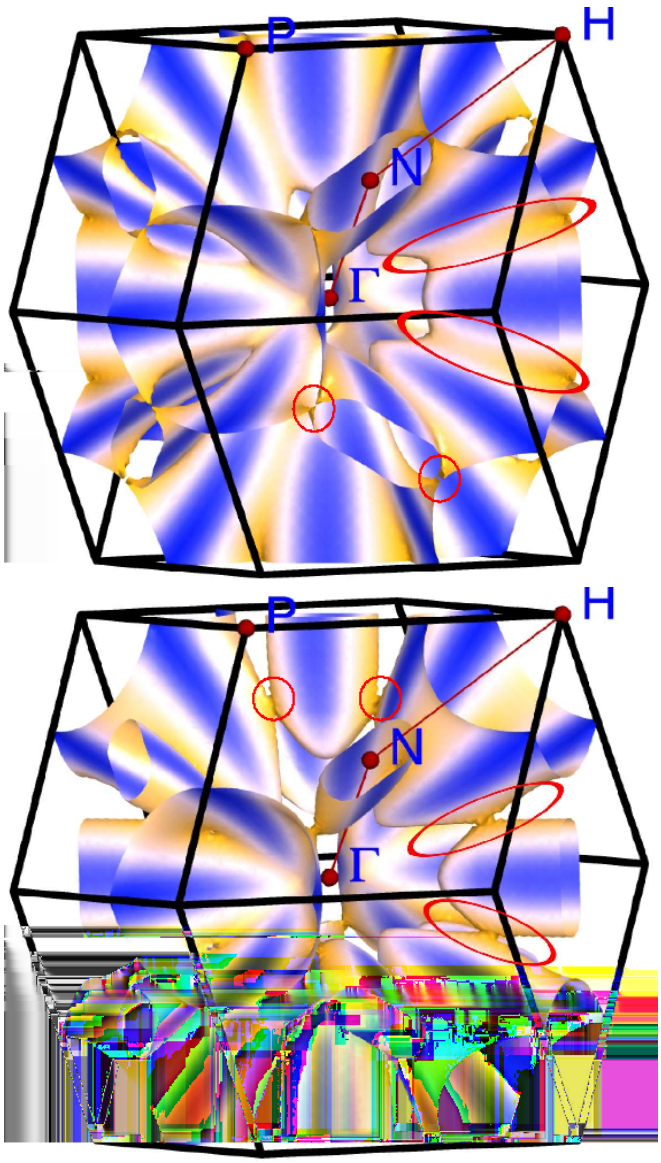

FIG. 7: Top: iso-energy contour from FPLO for the vHs at E=-0.43eV. Bottom: similarly for the vHs at E=-0.11 eV. The red circles pinpoint two of the symmetry related vHs in each case. The red ellipse outlines the region joined by the two van Hove singularities; two energy surfaces are "unzipped' as the energy increases between the two vHs. Color denotes the velocity, which ranges from zero (darkest tan, at the vHs) to 2.5×10^8 cm/s (deep blue).

A single frequency moment is sufficient, since the logarithmic, first, and second moments differ only at the 2% level; we denote this frequency Ω. Using a somewhat different value of Ω below would not change our conclusions.

From visual examination, the sheets of the constant energy surfaces at $E_F\pm\Omega$ do not differ much from the Fermi surfaces at E_F (see Fig. 7), the differences occurring in small pockets around Γ (not visible) and along a line connecting the two vHs. Inter-vHs scattering could be interesting: although it involves a small amount of phase (k-) space, it incorporates a disproportionate fraction of states with low to vanishing velocity. Possible complication from inter-vHs scattering and non-adiabatic processes lie beyond the scope of our discussion.

A. Formalism

It has been known since the work of Engelsberg and Schrieffer[32] and Shimojima and Ichimura[33] fifty years ago that, for a characteristic phonon frequency Ω in an interacting electron-phonon system, electron spectral density is spread from its noninteracting δ-function spike at E_k up to a few Ω. The spectral density arises from the electronic self-energy that is treated for superconducting systems by Eliashberg theory. When N(E) is slowly varying over a scale of a few Ω it is rare to notice the effects of such broadening except possibly in direct measurements where phonon sidebands may be observed in photoemission spectra. For situations as in H_3S where Bloch state character is slowly varying in energy but N(E) varies rapidly, the normally simple electron-phonon formalism becomes more challenging. Drozhov studied the effects of EPC in the vicinity of a vHs where Migdal's theorem is violated, and found severe renormalizations.[34] If these are confined to a very small phase space, however, the effects on most properties may be minor.

For the case of rapidly varying N(E) but neglecting violations of Migdal's theorem, the generalization of Eliashberg theory has been formulated and applied to the A15 compounds.[29,35] One feature that is distinctive in H_3S compared to most other EPC superconductors is that T_c is an order of magnitude higher, because the frequencies are comparably higher, and simple thermal broadening is correspondingly larger and requires attention. The second factor in common, and the important one, is that strong EPC causes an effective smearing of the electronic spectral density due to exchange of virtual phonons appearing in Migdal-Eliashberg theory – excitations described by the electron Green's function are part electron, part phonon. This broadening is given by the imaginary part of the interacting electronic Green's function

$$G_k^{-1}(\omega) \;=\; \omega - [E_k - \mu(T)] - M_k(\omega;T) - i\Gamma_k(\omega;T). \quad (3)$$

Here E_k is the DFT band energy, $\mu(T)$ is the chemical potential, and M and Γ are the real and imaginary parts of the phonon-induced self-energy.

The spectral density $A(\omega)$ is the interacting analog of the band DOS N(E):

$$\begin{aligned} A(\omega) \;&=\; \sum_k A_k(\omega) = \frac{1}{\pi}\sum_k |ImG_k(\omega)| \qquad (4)\\ &=\; \frac{1}{\pi}\sum_k \frac{\Gamma_k(\omega)}{[\omega-(E_k-\mu)-M_k(\omega)]^2+\Gamma_k(\omega)^2}\\ &\to\; \int d\xi \frac{\Gamma/\pi}{(\omega-\xi)^2+\Gamma^2} N(\xi). \end{aligned}$$

In the last expression the Brillouin sum has been converted into an energy integral by inserting $\int dE\delta(E - E_k)$=1, assuming that only E_k (and not wavefunction character, hence not M or Γ) depends on k near E_F, and $\xi_k = \varepsilon_k - \mu + M(k, \xi_k)$ is the quasiparticle energy. This simplification is usually fine for electron-phonon coupling in a standard Fermi liquid, as wide-band H_3S appears to be.

There is strong rearrangement of spectral density even before this smearing effect of electron damping Γ. For temperatures and frequencies ω up to the order of the characteristic phonon energy Ω or more, the behavior of the real part M_k is linear $dM_k/d\omega = -\lambda_k$, where λ_k is the EPC strength at k whose average over the Fermi surface is λ. The equation for ξ_k in the previous paragraph then gives for the quasiparticle energy

$$\xi_k = \frac{E_k - \mu}{1 + \lambda_k}. \tag{5}$$

This equation expresses the phonon-induced Fermi surface mass enhancement $1 + \lambda_k$, and $(1 + \lambda_k)^{-1}$ is the quasiparticle strength, i.e. the fraction of the electron's δ-function spectral density at ξ_k and whose average in H_3S is 1/3 ($\lambda \approx 2$). Two-thirds of the spectral weight is spread from the quasiparticle energy ξ_k by up to a few times Ω. This is a serious redistribution of weight that we cannot treat in any detail without explicit solution for the Eliashberg self-energy on the real axis.

Notwithstanding the complications, in an interacting system the thermal distribution function containing all complexities can be handled formally to provide insight into this "varying N(E)" kind of system. The interacting thermal distribution (state occupation) function $f(E_k)$ is defined as the thermal expectation of the number operator n_k

$$\begin{aligned} f(E_k) &= T\sum_{-\infty}^{\infty} G_k(i\omega_n)e^{i\omega_n\eta} \\ &= \int_{-\infty}^{\infty} d\omega f_\circ(\omega)A(E_k,\omega), \end{aligned} \tag{6}$$

where the Matsubara sum with positive infinitesimal η has been converted into an integral in the last expression and $f_\circ(E)$ is the (non-interacting) Fermi-Dirac distribution. The k-dependence of M_k and Γ_k are considered to be weak and replaced by a Fermi surface average. The interacting distribution function can be expressed as the non-interacting one broadened by[35] $\Gamma_k(\omega)$ as N(E) is broadened in Eq. (4).

Several thermal properties can be formulated[35] in terms of the interacting (broadened and in principle mass renormalized) density of states $\mathcal{N}(E)$. Returning to single particle language, the spectral density at E_F is approximately

$$\mathcal{N}(E_F) = \int dE \frac{\Gamma/\pi}{(E - E_F)^2 + \Gamma^2} N(E). \tag{7}$$

For energies a few Ω around E_F the extension $E_F \to E$ to give $\mathcal{N}(E)$ will be reasonable. Then, returning to the distribution function, the total electron number can be written[35] in two ways

$$N_{el} = \int dE f(E)N(E) = \int d\omega f_\circ(\omega)\mathcal{N}(\omega), \tag{8}$$

illustrating that interaction effects can be exchanged between the distribution function and, in this instance, the interacting and non-interacting density of states. Thus in a region around E_F the spectral density is the band density of states broadened by a Lorentzian of halfwidth Γ.

B. Thermal and phonon smearing in H_3S

We now estimate the impact of this spectral density smearing for H_3S using the Wien2k result for N(E). The mass renormalization effects (from the real part of the self-energy) Migdal theory are outlined in Appendix D but will be disregarded here, leaving our estimate as an *underestimate* of the effect of smearing. Investigation of the (Migdal) self-energy equations (*i.e.* in the normal state) gives the quasiparticle inverse decay rate via phonons over most of the relevant energy range,[28,29,32] for an Einstein model, as

$$\Gamma \approx \pi\lambda\Omega[n_B(\Omega) + \frac{1}{2}] \tag{9}$$

For H_3S the characteristic frequency Ω is in the ballpark of $\Omega \approx 1300$ K (see above). Since we are interested only in relative values of quantities affected by smearing, we will not distinguish ω_{log} from ω_2, etc.

With the choice of μ^*=0.15, a value of λ=2.17 is necessary to give the observed T_c=200K, which also is in the range that has been quoted as resulting from DFT calculations. At 200 K, the Bose-Einstein thermal distribution n_B gives a negligible fraction of phonons excited: $n_B(\Omega) \sim 10^{-4}$. Thus

$$\Gamma = \frac{\pi}{2}\lambda\Omega = 5 \times 10^3\ K = 0.38\ \text{eV}, \tag{10}$$

the halfwidth is proportional to the product $\lambda\Omega$. This smearing in Eq. (6) arises from the virtual excitation of phonons that provides the coupling, even at low T_c where phonons are not excited. We note that zero-point vibrations do not scatter electrons; sharp Fermi surfaces survive strong electron-phonon coupling, with de Haas – van Alphen oscillations remaining visible, and the resistivity $\rho(T) \to 0$ at $T \to 0$.

Figure 8 shows three curves: the calculated (Wien2k) static lattice N(E) from Fig. 2, the thermally broadened version at 200 K, and the virtual phonon broadened DOS with halfwidth Γ=0.38 eV from above. The thermal broadening function is the derivative $-df_\circ(E - E')/dE$ with half width of about $\pi k_B T = 625$ K = 55 meV. This

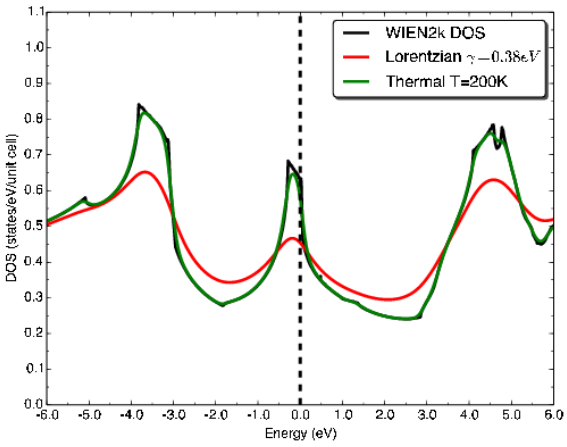

FIG. 8: H_3S density of states without broadening (black line, Wien2k DOS), with thermal broadening at 200 K (green line, which is hard to distinguish from the unbroadened one), and the virtual phonon broadened effective DOS N(E) using a Lorentzian halfwidth of 0.38 eV (red line). Note the large drop in the value at the Fermi energy (dashed vertical line).

thermal broadening at 200 K is minor on the scale of interest, reducing the effective value of N(E_F) slightly. The phonon broadening however is severe, with the peak value of 0.70/eV-f.u. for N(E) dropping by 37%. The unbroadened value N(E_F) of 0.64 states/eV-f.u. is lowered by nearly 1/3, to 0.45 states/eV-f.u. The effect of the shift of the chemical potential is secondary when broadening is so large.

C. Implications for the theory of H_3S

The Eliashberg equations including the energy dependence[28,29] of N(E) indicate that it is this 1/3 reduced value of N(E_F) that should be used with the standard implementation to get a good estimate of λ, the superconducting gap, and T_c. The impact of experiment/theory agreement for H_3S is substantial and negative: the spectral function $\alpha^2F(\omega)$, proportional to $N(E_F)$, is reduced by 1/3 by EPC. The naive value of $\lambda \approx 2.17$ becomes, after reducing by 1/3, λ=1.45. The phonon frequency moments, which involve α^2F/λ, seem at this stage to remain unchanged; we return to this point below.

We have evaluated the magnitude of this phonon broadening correction on T_c using the Allen-Dynes equation,[37] taking the representative values for H_3S of the phonon moments to be $\Omega = 1300$ K and μ^*=0.15. For λ=2.17, T_c = 200 K; for the 1/3 reduced value λ=1.45, T_c=130 K. The agreement between theory and experiment is strongly degraded. It is worthy of note that H_3S happens to be in a nearly linear regime of $T_c(\lambda)$, where a reduction of λ by 1/3 results in a decrease of T_c by nearly 1/3. We note that the corresponding strong coupling factor f_1 in the Allen-Dynes parametrization is 1.13 (1.07); f_1 is the crucial improvement of the Allen-Dynes equation over the McMillan equation and seems sometimes for hydrogen sulfides to have been neglected.

What this comparison implies is that theory-experiment agreement for T_c is not as good as has seemed, since taking phonon smearing into account, theory would only be predicting of the order of 2/3 of the "constant $N(E_F)$" value. It should be noted that this 1/3 reduction factor depends on the accurate calculation of $N(E)$, for which we have used the Wien2k spectrum. With the FPLO result for the DOS, $N(E_F)$ is lower and thus the effect of smearing will be smaller.

A few papers have reported calculations of the band structure and of N(E), and some studies have reported λ, but little attention has been given to the value of N(E_F), which is sensitive to method and computational procedures. At 200 GPa (a=5.6 a.u.) Papaconstantopoulos *et al.* quote 0.51/eV-f.u.; Duan *et al.* obtain[36] 0.41/eV-f.u.; Bianconi and Jarlborg report 0.50/eV-f.u. (their table numbers must be per cubic cell). Our Wien2k and FPLO values are 0.64 (0.42)/eV-f.u. respectively, indicating that even all-electron full potential methods can differ.

The point is that in conventional Eliashberg theory – constant N(E) on the phonon scale – λ is proportional to N(E_F), and the values that have been used are sensitive to methods and cutoffs (depending on method, see above), but more seriously they are obtained from unbroadened N(E). Because of this, the reported values of λ and hence T_c are quantitatively uncertain, assuming they are converged BZ integrals. And on this point, McMahon and Ceperley[14] and Akashi *et al.*[16] have discussed the various challenges in reaching convergence, before even confronting the energy variation question. The (unsmeared) prediction of $T_c \approx$ 200 K indicates that improved theory, by taking into account phonon broadening, would give a substantially reduced critical temperature.

Flores-Livas *et al.* have recognized the issue of the variation of N(E) on the scale of the phonon frequencies. In their implementation of density functional theory for superconductors (DFTSC), this variation is accounted for. They reported, for their calculation of N(E) (details were not reported), taking into account the variation resulted in a 16% decrease in T_c, from 338 K to 284 K in their calculation. Their methods also involve calculation of μ^* that is not treated in the Eliashberg form as well as other methodological differences, and these differences make direct comparison with other reports difficult. Still, the relative effects of energy variation of N(E) are clear.

This DOS variation issue extends to the calculation of phonon frequencies. The phonon self-energy involves electron-phonon scattering in which a phonon is absorbed, scattering an electron from $E_k < E_F$ to $E_k + \omega_q > E_F$. Most methods of calculating phonon frequencies do not include effects of the density of available initial or final states in this energy region being variable. Thus cal-

culation of phonon spectra will need to be re-evaluated for situations such as that imposed by H_3S, and the associated non-adiabatic corrections considered.

V. ROUTES TO HIGHER CRITICAL TEMPERATURE

The foregoing section indicates that 200 K superconductivity has been achieved with an effective DOS around $\mathcal{N}(E_F) \approx 0.44$/eV-f.u. compared to a peak value between the two vHs around 0.7/eV-f.u. This means as mentioned above that the theory needs refining, as already noted by Flores-Livas *et al.*, to determine just how much is understood quantitatively and what features may require more attention.

This difference in N(E) versus $\mathcal{N}$(E) has larger and much more positive implications. The fact that a reduced effective value of $\mathcal{N}(E_F)$ should be used for H_3S also provides the glass-half-full viewpoint: a much larger value of $\mathcal{N}(E_F)$ and therefore T_c may be achievable in this or similar systems. Suppose that the two vHs can be moved apart, each by (say) 0.5 eV, leaving a value $N(E_F)$ ≈0.7/eV-f.u. between. Then the Lorentzian smearing will have much less effect. There is also the question of increasing the *magnitude* of N(E) at the peak, *i.e.* $N(E_{vhs})$. This value depends on the effective masses at the vHs, but also on the volume of the region in which the quadratic effective mass representation holds. If it holds in an ellipsoidal region defined by

$$\sum_j \frac{\hbar^2 k_j^2}{2m_j} < G_c^2, \tag{11}$$

the DOS from this region is

$$N(E) \propto m_{th}^{3/2}[\alpha G_c - \beta \frac{|E - E_{vhs}|}{G_c} + ...], \tag{12}$$

where α and β are numbers of order unity. The value $N(E_{vhs})$ at the vHs is proportional to the thermal mass and to the radius G_c of the region of quadratic dispersion, and the decrease away from the vHs (the second term) is inversely proportional to G_c. There will be additional smooth contributions from outside this region, of course. However, increasing m_{th} and the region of quadratic dispersion is favorable for increasing $\mathcal{N}(E)$ in the vHs region, and hence increasing T_c. These observations seems to implicate the *topology* of the Fermi surfaces, rather than more conventional electronic structure characteristics such as relative site energies and hybridization strengths.

Numerical examples are illuminating. Suppose that the DOS peak can be widened so that $\mathcal{N}(E_F) \approx N(E_F)$ = 0.70/ev-f.u. as outlined just above, rather than the reduced effective value of 0.45eV/f.u. that gives, experimentally, T_c=200K. With Ω = 1300 K and μ^*=0.15 as above, λ_{exp}=2.17 is required to account for T_c = 200K. For a 0.70/0.44 = 1.55 larger value of $N(E_F)$, λ=3.38 and we find T_c=277K – room temperature in a cool room. The increase in effective $\mathcal{N}(E_F)$ we have assumed is ambitious but not outlandish, given the calculated spectrum of $Im\bar{3}m$ H_3S. It is clearly worthwhile to explore other H-rich compounds for higher critical temperatures.

Of course, the increase in $\mathcal{N}(E_F)$ will give additional renormalization (softening) of the phonons. However, the modes are very stiff even with λ=2.1, so this may not be a major effect. Note that decreasing Ω increases λ but decreases the energy scale prefactor in T_c, one reason why increasing λ by decreasing frequencies is rarely a profitable means of increasing T_c. If Ω, the prefactor in the Allen-Dynes T_c equation, is softened by 10% without change in matrix elements, λ increases by 20% while T_c increases by only 4%. Evidently softening of hard phonons is a minor issue when looking for higher T_c in this range of λ. This behavior was formalized by Allen and Dynes,[37] who obtained the rigorous strong coupling limit

$$T_c \to 0.18\sqrt{\lambda < \omega^2 >} = 0.18\sqrt{N(E_F) < I^2 > /M}, \tag{13}$$

where ω is expressed in kelvins. The last expression is strictly true only for an elemental superconductor, think of the electron-ion matrix element I and mass M as those of H for H_3S.

VI. SUMMARY

In this paper we first addressed the electronic structure and especially the delicate van Hove singularity induced spectrum, bonding characteristics and effect of S, and the charge density of states near the Fermi level, more directly than has been done before. The occurrence of two closely spaced van Hove singularities is definitely a central issue for the properties of H_3S. We list some of the main points.

• At the most basic level, why is H_3S superconducting at 200 K? It is because both λ is large but, more importantly, the characteristic phonon frequency Ω is very high. This reminds one of the Allen-Dynes limit for strong coupling,

$$T_c \to 0.18\sqrt{\lambda\Omega^2} \to 0.18\sqrt{N(E_F) < I^2 > /M}. \tag{14}$$

Though not yet in this limit, this provides the right picture – one can check that keeping all fixed except for Ω and then varying it, the change in T_c is minor because the change in prefactor $T_c \propto \Omega$ is compensated by $\lambda \propto \Omega^{-2}$.

• Sulfur $3p$ states hybridizing with hydrogen $1s$ is crucial in producing the strong large scale structure in N(E) within ±5 eV of the Fermi level, and in leaving E_F at the top of a peculiarly sharp peak between two vHs. The van Hove points on the constant energy surfaces that define the peak in N(E) were identified, finding they lie on opposite ends of a line of Fermi surface "ripping apart" with energy varying between the two van Hove singularities.

This region of very low velocity electrons affects a significant fraction of the zone. It is unclear how replacing S with other elements will affect the electronic structure near E_F, but small changes may have large effects. Ge *et al.* have noted that alloying 7-10% of P with S moves E_F to the peak in N(E), within the virtual crystal approximation which does not account for alloy disorder broadening. In any case, strong coupling smearing as discussed here will nullify this apparent gain.

• The fine structure and energy variation of $N(E)$ near the Fermi level must be taken into account to obtain quantitative results for α^2F, λ, and T_c. The energy dependence of N(E) may even affect calculation of phonon frequencies, though this is untested so far.

• The closely spaced van Hove singularities very near the Fermi level have been shown to have significance, both on the detailed theory of H_3S but, as importantly, on the question of whether T_c can be increased in related materials. Sulfur and the specific $Im\bar{3}m$ structure are important for high T_c though other elements will need to be studied to learn more about precisely why.

• The prospect for increased T_c is affirmative – it will require only evolutionary changes of the electronic structure to achieve room temperature superconductivity, though the road to this goal requires study, and additional insight into the origins of van Hove singularities may be important. Increasing the vHs effective masses, or increasing the volume within which quadratic dispersion holds, will increase N(E) at the vHs energy. Structural or chemical changes that affect the electronic structure rather modestly may lead to significant increase in the effective (broadened) density of states at E_F. Other studies have suggested that substitution of some sulfur with chemically related elements may increase T_c. Altogether, the prospects of achieving increased critical temperatures are encouraging.

• An issue that is almost untouched is a deeper understanding, or rather an understanding at all, of electron-ion matrix elements $< I_H^2 >$ – what contributes to strong electron-H atom scattering, and what degrades this scattering. These matrix elements are the same that determine resistivity in the normal state; notably most of the best superconductors have high resistivities. Further study should address the EPC matrix elements.

VII. ACKNOWLEDGMENTS

We acknowledge helpful discussions with, and comments on the manuscript from, A. S. Botana, B. M. Klein, M. J. Mehl, and D. A. Papaconstantopoulos. Our research used resources of the National Energy Research Scientific Computing Center (NERSC), a DOE Office of Science User Facility supported by the Office of Science of the U.S. Department of Energy under Contract No. DE-AC02-05CH11231. This work was supported by National Science Foundation award DMR-1207622.

* Electronic address: wepickett@ucdavis.edu

[1] A. P. Drozdov, M. I. Eremets, and I. A. Troyan, Conventional superconductivity at 190 K at high pressures, arXiv:1412.0460.

[2] A.P. Drozdov, M. I. Eremets, I. A. Troyan, V. Ksenofontov, S. I. Shylin, Conventional superconductivity at 203 K at high pressures, arXiv:1506.08190.

[3] A.P. Drozdov, M. I. Eremets, I. A. Troyan, V. Ksenofontov, S. I. Shylin, Conventional superconductivity at 203 K at high pressures in the sulfur hydride system, Nature **525**, 73 (2015). http://dx.doi.org/10.1038/nature14964

[4] D. Duan, Y. Liu, F. Tian, D. Li, X. Huang, Z. Zhao, H. Yu, B. Liu, W. Tian, and T. Cui, Pressure-induced metallization of dense $(H_2S)_2H_2$ with high-T_c superconductivity, Sci. Rep. **4**, 6968 (2014).

[5] M. Einaga, M. Sakata, T. Ishikawa, K. Shimizu, M. Eremets, A. Drozdov, I. Troyan, N. Hirao, and Y, Ohishi, Crystal structure of 200 K-superconducting phase of sulfur hydride system, arXiv:1509.03156.

[6] I. Errea, M. Calandra, C. J. Pickard, J. Nelson, R. J. Needs, Y. Li, H. Liu, Y. Zhang, Y. Ma, and F. Mauri, High-pressure hydrogen sulfide from first principles: a strongly anharmonic phonon-mediated superconductor, Phys. Rev. Lett. **114**, 157004 (2015).

[7] D. A. Papaconstantopoulos, B. M. Klein, M. J. Mehl, and W. E. Pickett, Cubic H_sS around 200 GPa: an atomic hydrogen superconductor stabilized by sulfur, Phys. Rev. B **91**, 184511 (2015).

[8] N. Bernstein, C. S. Hellberg, M. D. Johannes, I. I. Mazin, and M. J. Mehl, What superconducts in sulfur hydrides under pressure and why, Phys. Rev. B **91**, 060511(R) (2015).

[9] C. Heil and L. Boeri, Influence of bonding on superconductivity in high-pressure hydrides, Phys. Rev. B **92**, 060508 (2015).

[10] J. A. Flores-Livas, A. Sanna, and E. K. U. Gross, High temperature superconductivity in sulfur and selenium hydrides at high pressure, arXiv:1501.06336.

[11] N. W. Ashcroft, Metallic hydrogen: a high-temperature superconductor? Phys. Rev. Lett. **21**, 1748 (1968).

[12] N. W. Ashcroft, Hydrogen dominant metallic alloys: high temperature superconductors? Phys. Rev. Lett. **92**, 187002 (2004).

[13] D. A. Papaconstantopoulos and B. M. Klein, Electron-phonon interaction and superconductivity in metallic hydrides, Ferroelectrics **16**, 307 (1977).

[14] J. M. McMahon and D. M. Ceperley, High temperature superconductivity in atomic metallic hydrogen, Phys. Rev. B **84**, 144515 (2011).

[15] D. J. Scalapino, J. R. Schrieffer, and J. W. Wilkins, Strong coupling superconductivity. I. Phys. Rev. **148**, 263 (1966).

[16] R. Akashi, M. Kawamura, S. Tsenuyuki, Y. Nomura, and R. Arita, First principles study of the pressure and crystal-structure dependence of the superconducting transition temperature in compressed sulfur hydrides, Phys. Rev. B **91**, 224513 (2015).

[17] A. Bianconi and T. Jarlborg, Superconductivity above the

lowest Earth temperature in pressurized sulfur hydride, EPL **112**, 37001 (2015).
[18] Y. Li, J. Hao, H. Liu, Y. Li, and Y. Ma, The metallization and superconductivity of dense hydrogen sulfide, J. Chem. Phys. **140**, 174712 (2014).
[19] J. Labbé, S. Barišić, and J. Friedel, Strong-coupling superconductivity in V_3X type of compounds, Phys. Rev. Lett. **19**, 1039 (1967).
[20] R. S. Markiewicz, van Hove singularities and high-T_c superconductivity: a review. Intl. J. Mod. Phys. B **5**, 2037 (1991).
[21] A. A. Abrikosov, Ginzburg-Landau equations for the extended saddle-point model, Phys. Rev. B **56**, 446 (1997).
[22] P. Blaha, K. Schwarz, G. K. H. Madsen, D. Kvasnicka, and J.. Luitz, WIEN2k, an augmented plane wave plus local orbital program for calculating crystal properties, (Vienna University of Technology, Vienna, Austria, 2001). ISBN 3-9501031-1-2.
[23] K. Koepernik and H. Eschrig, Full potential nonorthogonal local orbital minimum basis band structure scheme, Phys. Rev. B **59**, 1743 (1999).
[24] J. P. Perdew, K. Burke, and M. Ernzerhof, Generalized Gradient Approximation Made Simple, Phys. Rev. Lett. **77**, 3865 (1996).
[25] Y. Ge, F. Zhang, and Y. Uao, Possible superconductivity approaching the ice point, arXiv:1507.08525.
[26] N. A. Mecholsky, L. Resca, I. L. Pegg, and M. Fornari, Density of States for Warped Energy Bands, arXiv:1507.04031. See Eq. (28).
[27] A. P. Durajski, R. Szcześmoal. and Y. Li, Non-BCS thermodynamic properties of H_2S superconductor, Physica C **515**, 1 (2015).
[28] W. E. Pickett, Effect of a varying density of states on superconductivity, Phys. Rev. B **21**, 3897 (1980).
[29] W. E. Pickett, Generalization of the theory of the electron-phonon interaction: thermodynamic formulation of superconducting- and normal-state properties, Phys. Rev. B **26**, 1186 (1982).
[30] B. Mitroviić and J. Carbotte, Superconducting T_c for the separable model of $(\varepsilon, \varepsilon')$ variation in $\alpha^2F(\varepsilon, \varepsilon'; \Omega)$, Phys. Rev. B **28**, 2477 (1983).
[31] R. J. Radtke and M. R. Norman, Relation of extended van Hove singularities in High temperature superconductivity with strong-coupling theory, Phys. Rev. B **50**, 9554 (1994).
[32] S. Engelsberg and J. R. Schrieffer, Coupled Electron-Phonon System, Phys. Rev. **131**, 993 (1963).
[33] K. Shimojima and H. Ichimura, Spectral Weight Function and Electron Momentum Distribution in the Normal Electron-Phonon System, Prog. Theor. Phys. **43**, 925 (1970).
[34] Yu. P. Drozhov, Electron-phonon interaction in the vicinity of the van Hove critical point, Phys. Stat. Sol. (b) **98**, 781 (1980).
[35] W. E. Pickett, Renormalized thermal distribution function in an interacting electron-phonon system, Phys. Rev. Lett. **48**, 1548 (1982).
[36] D. Duan, private communication.
[37] P. B. Allen and R. C. Dynes, Transition temperature of strong-coupled superconductors reanalyzed, Phys. Rev. B **12**, 905 (1975).